

# Formation of Differential-Drive Vehicles with Field-of-View Constraints for Enclosing a Moving Target

Gonzalo López-Nicolás, Miguel Aranda and Youcef Mezouar

**Abstract**—An emerging application of multirobot systems is the monitoring of a dynamic event. Here, the goal is to enclose and track a moving target by attaining a desired geometric formation around it. By considering a circular pattern configuration for the target enclosing, the multirobot system is able to perform full perception of the target along its motion. In the proposed system, the robots rely only on their onboard vision sensor without external input to complete the task. The key problem resides in overcoming the motion and visual constraints of the agents. In particular, differential-drive robots with limited sensing, that must maintain visibility of the moving target as it navigates in the environment, are considered. A novel approach to characterize the motion of the robots in the formation that allows to enclose and track the target while overcoming their limited field of view (FOV) is presented. The proposed approach is illustrated through simulations.

## I. INTRODUCTION

Research on multirobot systems has become a very active topic in the recent years due to the ability of these systems to collectively carry out complex tasks and because of the great variety of theoretical and practical challenges they raise. Here, within the field of multiagent formation control, we focus on the particular problem of target enclosing [1]. In this problem, the team of robots is required to maintain a particular formation around a target. Usually, circular formations are considered for the enclosing task in 2D space [2], [3]. We can also find encirclement in 3D space [4], or enclosing with arbitrary formations in 3D space [5]. Related works to this task are [6], where a distributed method based on local sensing is presented, and [7], where distributed target enclosing is performed with a coordinate-free approach.

More specifically, we consider the problem of enclosing a moving target to be perceived by means of multiple sensors (i.e. multiple robots) to obtain, e.g., a complete representation of this target. Some previous approaches rely on some external input to complete the task [8], [9]. However, this type of systems is restricted to limited environments, and cannot be used to capture the dynamic target following long paths. Therefore, in the system considered here the robots must rely only on their independent onboard sensors. This problem

of formation control in the context of target tracking was addressed using consensus algorithms to perform flocking [10], or by filming a target through flying cameras [11].

Existing approaches usually observe the target through vision sensors [3], [9], [10], [11]. We too consider here that each robot of the formation carries a camera as a sensor. A main drawback of standard cameras for the considered task is their limited field of view (FOV). This constraint is also hardened by the differential-drive motion constraints of the mobile platforms assumed in this work. The problem of nonholonomic robot navigation while maintaining visibility of a fixed landmark using an onboard camera with a limited FOV was tackled in [12] and [13]. Optimality of the paths that are achieved was later addressed in [14], [15] and a visual servo control system based on homographies was also proposed in [16] by following optimal paths while taking care of the visual sensor constraints. These works model the camera FOV as a symmetric and planar cone aligned to the forward direction of motion. In [17], the synthesis of shortest paths with general FOV (e.g. side-looking sensors) was provided. The problem of finding collision-free paths in an environment with obstacles with both nonholonomic and field-of-view constraints was tackled in [18].

These previous works consider only one robot and a static target to maintain in the FOV. Control of multirobot systems with limited FOV was studied in [19] for a containment task. Connectivity and consensus analysis were provided, although single-integrator robots are assumed and the goal is to converge to a static configuration, preventing the application of the proposed method to a moving target. The work in [20] addressed the problem of cooperative coordination of leader-follower formations of mobile robots with visibility and communication constraints. Proposal in [20] aims at controlling a tractor-trailer formation in the presence of obstacles with forward-looking sensors rather than performing full perception of the target.

In this paper, we consider a team of mobile robots with differential-drive motion constraints. Each robot carries a camera, not necessarily forward-looking, with limited FOV. We seek full perception of the target, which implies that all the robots must maintain visibility of the target from different predefined points of view around this target. We consider a circular pattern configuration to enclose the target that must be maintained in the FOV of each robot. In order to perform full perception of the target, we present a new approach to address this task. In particular, we characterize the motion of the robots in the formation that achieves the goal of enclosing and tracking the target while overcoming their limited FOV.

G. López-Nicolás is with Instituto de Investigación en Ingeniería de Aragón. Universidad de Zaragoza, Spain. gonlopez@unizar.es

M. Aranda and Y. Mezouar are with Université Clermont Auvergne, CNRS, SIGMA Clermont, Institut Pascal, F-63000 Clermont-Ferrand, France. miguel.aranda@sigma-clermont.fr, youcef.mezouar@sigma-clermont.fr

This work was supported by Spanish Government/European Union Project DPI2015-69376-R (MINECO/FEDER), by Universidad de Zaragoza, Fundación Bancaria Ibercaja and Fundación CAI, by French Government research program Investissements d'avenir through the RobotEx Equipment of Excellence (ANR-10-EQPX-44), the LabEx IMobS3 (ANR17107LABX716701) and the FUI project Aerostrup.

## II. PROBLEM FORMULATION

Let us consider a moving target to be enclosed and tracked in  $\mathcal{R}^2$  with position  $\mathbf{q}_t(t) = (x_t(t), y_t(t))^T$  and orientation  $\phi_t(t) \in \mathcal{R}$  expressed in an arbitrary global reference frame. We assume that the target follows unicycle kinematics:

$$\dot{x}_t = v_t \cos \phi_t, \quad \dot{y}_t = v_t \sin \phi_t, \quad \dot{\phi}_t = \omega_t, \quad (1)$$

where  $v_t(t) \in \mathcal{R}$  and  $\omega_t(t) \in \mathcal{R}$  are the linear and angular velocity of the target. Here, we assume a strictly positive velocity  $v_t$ . We define the signed curvature of the target's trajectory as  $k_t(t) = \omega_t/v_t$  and the curvature  $\kappa_t(t) = |\omega_t/v_t|$ . In order for the tracking of the target to be feasible, we assume that the curvature of the target's trajectory is upper bounded by some  $\kappa_{t_{max}}$ . Therefore  $0 \leq \kappa_t \leq \kappa_{t_{max}} < \infty$ .

Let us also consider  $N$  robots in  $\mathcal{R}^2$  to generate the formation for enclosing and tracking the target. Their position and orientation are  $\mathbf{q}_i(t) = (x_i(t), y_i(t))^T$  and  $\phi_i(t) \in \mathcal{R}$ , with  $i = 1, \dots, N$ . These robots follow unicycle kinematics:

$$\dot{x}_i = v_i \cos \phi_i, \quad \dot{y}_i = v_i \sin \phi_i, \quad \dot{\phi}_i = \omega_i, \quad (2)$$

where  $v_i(t) \in \mathcal{R}$  and  $\omega_i(t) \in \mathcal{R}$  are the linear and angular velocities of the robots.

We choose a circular formation for enclosing the target. The shape of this formation can be represented by a regular polygon with  $N$  robots evenly distributed along the circumference. The size or scale of the formation is defined by its radius  $d_i = d(t)$ , with  $d$  of differentiability class  $C^2$  or higher. We consider the target is in the centroid of the circular formation. Then, the value of  $d$  is the same for all robots in the formation, equal to the distance of each robot to the target. Notice that this radius could be constrained in practice, for instance, to avoid collision with the target or to avoid a small target size in the image because of the distance:  $0 < d_{min} \leq d \leq d_{max} < \infty$ . The position of each robot in the circumference is defined by angle  $\theta_i \in [-\pi, \pi]$ , which is fixed for each robot, and defined anticlockwise from the  $x$ -axis of the local reference frame on the target. In particular, we have  $\theta_i = \pi(2i/N - 1)$  for  $i = 1, \dots, N$ . Then, the corresponding coordinates of each robot with respect to the moving target reference are

$$x_{0i}(t) = d \cos \theta_i, \quad \text{and} \quad y_{0i}(t) = d \sin \theta_i. \quad (3)$$

Each robot in the formation has a camera on board, which is fixed on the robot and pointing to the target. Note that if the robots have the same orientation as the target in the circular formation (see example in Fig. 1), then for robot at  $\theta_i$  the camera forms a fixed angle of  $(\theta_i - \pi)$  if  $\theta_i > 0$ , or  $(\theta_i + \pi)$  if  $\theta_i \leq 0$ , with respect to its forward motion direction.

The FOV of each camera is limited by angle  $\beta_i^{min} < 0$  and  $\beta_i^{max} > 0$ . For simplicity, we assume symmetric FOV ( $\beta_i = -\beta_i^{min} = \beta_i^{max}$ ) and that all the cameras have the same FOV ( $\beta_i = \beta$ ). For each robot, maintaining the target in its field of view implies keeping the projection of target  $\beta_{ti}(t)$  in robot's camera  $i$  such that  $\beta_{ti} \in [-\beta, \beta]$ .

**Problem:** Given a unicycle-type moving target (1) and a team of unicycle-type robots (2) enclosing that target

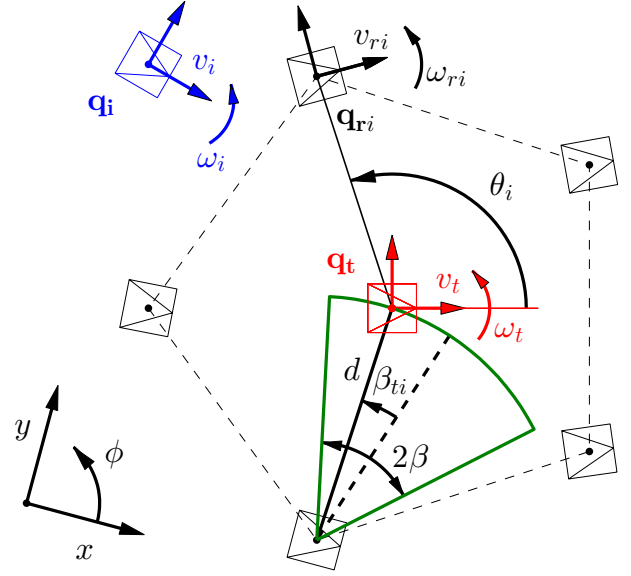


Fig. 1. Parameters involved in the problem formulation. Our contribution is the definition of the reference trajectories  $\mathbf{q}_{ri}$  for the robots  $\mathbf{q}_i$  to maintain a circular formation enclosing the target  $\mathbf{q}_t$  and maintaining FOV constraints. Each robot  $\mathbf{q}_i$  (only one is shown) will track its reference trajectory  $\mathbf{q}_{ri}$ . The FOV of the onboard fixed camera of one robot is also shown.

in circular formation, find an appropriate tracking strategy for the robots such that the geometry of the formation is maintained, i.e. the relative positions of the robots in the formation and the target are maintained, while guaranteeing that the target is always in the field of view of all onboard cameras, i.e.  $\beta_{ti} \in [-\beta, \beta]$ .

## III. CONSTRAINED REFERENCE TRAJECTORIES

Given the target velocities  $v_t$  and  $\omega_t$  or equivalently, the target path  $(x_t, y_t)$  and  $\phi_t$ , we next deduce the robots' path to track the moving target in rigid formation while taking into account the motion and visibility constraints.

### A. Reference tracking trajectories

The main problem is to find appropriate trajectories to be tracked by the robots of the formation. The task requires that the robots must maintain the formation geometry at any-time while keeping visibility constraints. Then, the problem resides in finding a suitable reference path for each robot, which is defined by its position  $\mathbf{q}_{ri}(t) = (x_{ri}(t), y_{ri}(t))^T$  and orientation  $\phi_{ri}(t) \in \mathcal{R}$ , with  $i = 1, \dots, N$ . In order to create feasible trajectories we impose unicycle kinematics:

$$\dot{x}_{ri} = v_{ri} \cos \phi_{ri}, \quad \dot{y}_{ri} = v_{ri} \sin \phi_{ri}, \quad \dot{\phi}_{ri} = \omega_{ri}, \quad (4)$$

where  $v_{ri}(t) \in \mathcal{R}$  and  $\omega_{ri}(t) \in \mathcal{R}$  are the linear and angular velocities that generate the reference trajectories to be tracked by the robots. Expressing the coordinates of each robot (3) with respect to the global reference frame gives the following vector:

$$\begin{pmatrix} x_{ri} \\ y_{ri} \end{pmatrix} = \begin{bmatrix} \cos \phi_t & -\sin \phi_t \\ \sin \phi_t & \cos \phi_t \end{bmatrix} \begin{pmatrix} x_{0i} \\ y_{0i} \end{pmatrix} + \begin{pmatrix} x_t \\ y_t \end{pmatrix} \quad (5)$$

which reduces to

$$\begin{aligned} x_{ri} &= x_t + d \cos(\phi_t + \theta_i) \\ y_{ri} &= y_t + d \sin(\phi_t + \theta_i) . \end{aligned} \quad (6)$$

Calculating the time derivative of this vector yields

$$\begin{aligned} \dot{x}_{ri} &= v_t \cos \phi_t - d \omega_t \sin(\phi_t + \theta_i) + \dot{d} \cos(\phi_t + \theta_i) \\ \dot{y}_{ri} &= v_t \sin \phi_t + d \omega_t \cos(\phi_t + \theta_i) + \dot{d} \sin(\phi_t + \theta_i) . \end{aligned} \quad (7)$$

The reference orientation is then obtained as follows

$$\tan \phi_{ri} = \dot{y}_{ri} / \dot{x}_{ri} . \quad (8)$$

In the following, we define the reference velocities  $v_{ri}$  and  $\omega_{ri}$  from (7) and (8). We consider two cases regarding the scale of the formation: the general case in which  $d$  is variable as previously defined, and the particular case in which  $d$  is set to a constant value.

### B. Variable formation scale: $d(t)$

On the one hand, the forward reference velocity for each robot is computed from (4) and (7) as follows

$$\begin{aligned} v_{ri}^2 &= (\dot{x}_{ri})^2 + (\dot{y}_{ri})^2 \\ &= d^2 \omega_t^2 + \dot{d}^2 + v_t^2 + 2 v_t (\dot{d} \cos \theta_i - d \omega_t \sin \theta_i) . \end{aligned} \quad (9)$$

On the other hand, the angular velocity from (4) and the time derivative of (8) yield

$$\begin{aligned} \omega_{ri} &= \omega_t + (\dot{d}^2 + d \dot{d} \dot{\omega}_t - d \ddot{d}) \omega_t / v_{ri}^2 \\ &+ (\dot{d} v_t \omega_t - d \dot{v}_t \omega_t + d v_t \dot{\omega}_t) \cos \theta_i / v_{ri}^2 \\ &+ (\ddot{d} v_t - \dot{d} \dot{v}_t) \sin \theta_i / v_{ri}^2 . \end{aligned} \quad (10)$$

Notice that there can be an indeterminate term in the computation of  $\omega_{ri}$  when  $v_{ri} = 0$ . This happens when

$$(d \omega_t = v_t \sin \theta_i) \quad \wedge \quad (\dot{d} = -v_t \cos \theta_i) , \quad (11)$$

or also in the trivial case  $v_t = \omega_t = \dot{d} = 0$ . The indeterminate terms tends to zero, so we have in this case  $\omega_{ri} = \omega_t$ .

The reference velocities given by in (9) and (10) guarantee that the robots maintain the formation while tracking the target, but there is still no guarantee of maintaining the moving target in the cameras' FOV. Next we obtain the analytical expression of the field of view constraint. Using (7) in (8) with some trigonometry yields

$$d \omega_t - \dot{d} \tan(\phi_{ri} - \phi_t - \theta_i) = \frac{v_t \sin(\phi_{ri} - \phi_t)}{\cos(\phi_{ri} - \phi_t - \theta_i)} . \quad (12)$$

Maintaining the target in the FOV of the camera sensors implies that  $-\beta \leq \phi_t - \phi_{ri} \leq \beta$ . Therefore, denoting  $\beta_{ri}(t) = \phi_t - \phi_{ri}$  in (12) yields

$$d \omega_t - \dot{d} \tan(-\beta_{ri} - \theta_i) = \frac{v_t \sin(-\beta_{ri})}{\cos(\beta_{ri} + \theta_i)} , \quad (13)$$

and solving for  $\beta_{ri}$  in (13) yields the following constraint

$$|\tan \beta_{ri}| = \left| \frac{d \omega_t \cos \theta_i + \dot{d} \sin \theta_i}{d \omega_t \sin \theta_i - \dot{d} \cos \theta_i - v_t} \right| \leq \tan \beta . \quad (14)$$

Respecting this previous constraint guarantees the target is always in the FOV of the cameras. However, this does not guarantee by itself that the reference trajectory is feasible for a unicycle robot. For instance, one could define an arbitrary strategy to choose the value of  $d$  satisfying (14), and then determine the value of  $\phi_{ri}$  from (12) on the one hand, and the values of  $(x_{ri}, y_{ri})$  from (6) on the other hand. However, the results may be incompatible with (8), i.e. not feasible. Thus, we require an appropriate strategy for defining  $d$ . In particular, the scale of the formation  $d$  and its derivative  $\dot{d}$  give the degrees of freedom needed to allow an appropriate reference tracking trajectory to guarantee keeping both motion and FOV constraints.

In particular, we may choose tentative values of  $d$ , and then determine  $(x_{ri}, y_{ri})$  and  $\phi_{ri}$  with (6), (8). Finally we check if these values satisfy constraint (14) for all  $i$ . If so, we found a valid solution, otherwise we iterate modifying the values of  $d$ . Thus, any reference trajectory (6), (8) with corresponding velocities (9) and (10), that obeys the constraint in (14), and follows an appropriate strategy for  $d$  (to be presented in section IV) is a suitable solution of the enclosing and tracking problem considered.

Notice that  $\beta_{ri}$  is the reference evolution of the target projection in the image corresponding to the reference trajectories  $(\mathbf{q}_{ri}, \phi_{ri})$ , and it will be the task of the tracking control to make  $\beta_{ti} = \beta_{ri}$  by following these reference trajectories.

### C. Constant formation scale: $d$ constant

Depending on the application, it may be interesting to study the case in which the scale of the formation is required to be fixed to a constant value. Considering  $d$  as a constant parameter, we obtain the reference linear velocity for each robot from (4) and (7) as

$$v_{ri}^2 = (\dot{x}_r)^2 + (\dot{y}_r)^2 = d^2 \omega_t^2 + v_t^2 - 2 d v_t \omega_t \sin \theta_i . \quad (15)$$

Angular velocity from (4) and the time derivative of (8) yield

$$\omega_{ri} = \omega_t + d (v_t \dot{\omega}_t - \dot{v}_t \omega_t) \cos \theta_i / v_{ri}^2 . \quad (16)$$

Notice again that there is an indeterminate term in the computation of  $\omega_{ri}$  when  $v_{ri} = 0$ . In this case of constant  $d$ , this happens when  $(d \omega_t = \pm v_t)$  with  $(\theta_i = \pm \pi/2)$ , or also in the trivial case with  $v_t = \omega_t = 0$ . Again, the indeterminate terms tends to zero and  $\omega_{ri} = \omega_t$ .

Next we proceed to obtain the analytical expression of the field of view constraint in the case of  $d$  constant. Using (7) in (8) with constant  $d$ , we obtain the following equation

$$d = \frac{v_t \sin(\phi_{ri} - \phi_t)}{\omega_t \cos(\phi_{ri} - \phi_t - \theta_i)} . \quad (17)$$

Taking into account the FOV constraint  $|\phi_t - \phi_{ri}| \leq \beta$  yields the following limit constraint

$$d \leq \left| \frac{v_t \sin(\pm \beta)}{\omega_t \cos(\pm \beta - \theta_i)} \right| \quad \text{for } i = 1, \dots, N . \quad (18)$$

This previous expression gives the maximum admissible value of  $d$  in order to keep FOV constraints. Using the inverse

value of the radius of the formation yields

$$\kappa = 1/d \geq \left| \frac{\omega_t \cos(\pm\beta - \theta_i)}{v_t \sin(\pm\beta)} \right| \quad \text{for } i = 1, \dots, N. \quad (19)$$

This must hold for all  $\theta_i$ , and for all the instantaneous target curvatures. Thus, the worst case occurs when  $\theta_i = \{\pm\beta, \pm\beta - \pi\}$  and the curvature is the maximum, i.e.:

$$\kappa_{max} = \max \left| \frac{\omega_t}{v_t \sin(\pm\beta)} \right|. \quad (20)$$

Choosing this value to define the scale of the formation as  $d = 1/\kappa_{max}$  guarantees that the target is always maintained in the FOV for all the robots. Notice that the computation of the maximum admissible radius of the formation involves the maximum curvature of the target's trajectory  $\kappa_{t_{max}}$ , whose knowledge is thus needed in advance.

#### IV. FORMATION TRAJECTORY STRATEGIES

From the previous constraints we now propose two different strategies to define particular reference trajectories in order to enclose and track the target while guaranteeing motion and FOV constraints. Note that as long as the curvature of the target's trajectory is upper bounded ( $\kappa_{t_{max}}$ ), the existence of suitable reference trajectories is guaranteed.

##### A. Constant scale formation

First strategy consists in choosing a constant scale of the formation as  $d = 1/\kappa_{max}$  (20). By doing so, we maximize the scale of the formation with a constant value from the constraint ( $d \leq 1/\kappa_{max}$ ). Therefore, notice that any smaller scale will also guarantee the FOV constraints, whereas a higher constant value of  $d$  will violate these constraints. This is the simplest strategy that guarantees maintaining the moving target in the FOV of the cameras. It can be noticed that the higher the curvature of the target's motion ( $\kappa_t$ ), the smaller the value of  $d$  has to be in order to keep FOV constraints. This means that sharp motions of the target imply sharp reactions of the robots. Then, for a given  $\beta$ , smaller scale in the formation allows more leeway for keeping the FOV during the motion and hence allowing for sharper motions of the target. On the other hand, when the value of  $\kappa_t$  is low, e.g. the target follows a straight line, the scale of the formation can be arbitrarily high.

##### B. Variable scale formation

Another strategy we propose is based on increasing as much as possible the distance between the robots of the formation and the target. The previous strategy defines a constant value of  $d$ . This value is the maximum admissible without violating the FOV constraints when target reaches  $\kappa_{t_{max}}$ , but  $d$  can still be increased when  $\kappa_t < \kappa_{t_{max}}$  while maintaining FOV constraints. This may be interesting for example from a practical point of view in terms of maximising the safety distance between robots to prevent collisions, or to provide additional degrees of freedom to select an optimal distance from the visual sensor to the target.

Regarding the FOV constraints, we find upper and lower bounds to the value of  $d$  (or  $\kappa = 1/d$  indistinctively). In

particular, in terms of  $\kappa$ , there is a constant upper bound given by  $\kappa_{max}$  and there is a lower bound provided by (14). Here, we exploit the constant  $d$  constraint used in the previous strategy to be used in this new strategy. Notice that values over the constant upper bound also keep the FOV constraints, but we enforce this upper bound of  $\kappa$  (lower bound of  $d$ ) since this strategy aims to increase  $d$  as much as possible. Regarding the lower bound of  $\kappa$  along the time, it is defined by considering in (14) the case where the target is in the limit of the FOV (i.e. when  $|\beta_{ri}| = \beta$ ). Therefore, any valid reference trajectory is constrained between the value provided by (20) which limits the scale of the formation when the curvature of the target is maximum, and the value given by (14) which is the scale for which the target is in the limit of the FOV. Note that the constraints imply selecting an appropriate value not only for  $d$  but also for its derivative  $\dot{d}$ . In order to define  $d$ , we propose to use Gaussian type functions:

$$\kappa_g = 1/d_g = a \exp\left(-\frac{(t-b)^2}{2c^2}\right), \quad (21)$$

with  $a$ ,  $b$ ,  $c$  real constants, and  $t$  the time. We choose Gaussian functions inspired by the optimal paths presented in [14] which consisted in exponential functions. Although the smoothness of Gaussians is very appropriate for our task, note that any other function satisfying the presented constraints is valid.

Here, we propose to define a set of Gaussians in sequential intervals of time (depending on the target motion evolution) evolving within (20) and (14). The upper value of the Gaussians will reach  $\kappa_{max}$  when necessary (when  $\kappa_t$  is maximum) and will be reduced towards (14) by letting the target projection get as close as possible to the FOV limit.

#### V. SIMULATIONS

Several simulations are provided to illustrate the behaviour of the approach presented. In all the examples we consider a team composed by  $N = 5$  agents, forming consequently a regular pentagon. The required circular formation is depicted in Fig. 1. The FOV of each camera is represented with a wedge. In these examples, we consider  $\beta = 30$  deg.

The reference trajectories and values of  $d$  to fulfill the task are computed with the presented approach. Given the computed reference trajectories (6), we perform standard tracking control. Notice that standard tracking approaches usually assume that the target velocity is a bounded differentiable function whose derivative is also bounded and which does not tend to zero with time. In order to compute its motion commands, each robot needs the estimation of its relative position and orientation with respect to the target. Regarding the strategy in section IV-A, the value of  $\kappa_{t_{max}}$  needs to be known in advance, whereas the strategy in section IV-B also requires to know in advance the full trajectory of the target.

Simulation in Fig. 2 presents two examples of enclosing and tracking a target with ellipsoidal motion and 8-shape motion. There are three cases shown. The first one shows the motion of the formation with a constant value of  $d = 10$  m, which is higher than the maximum that guarantees

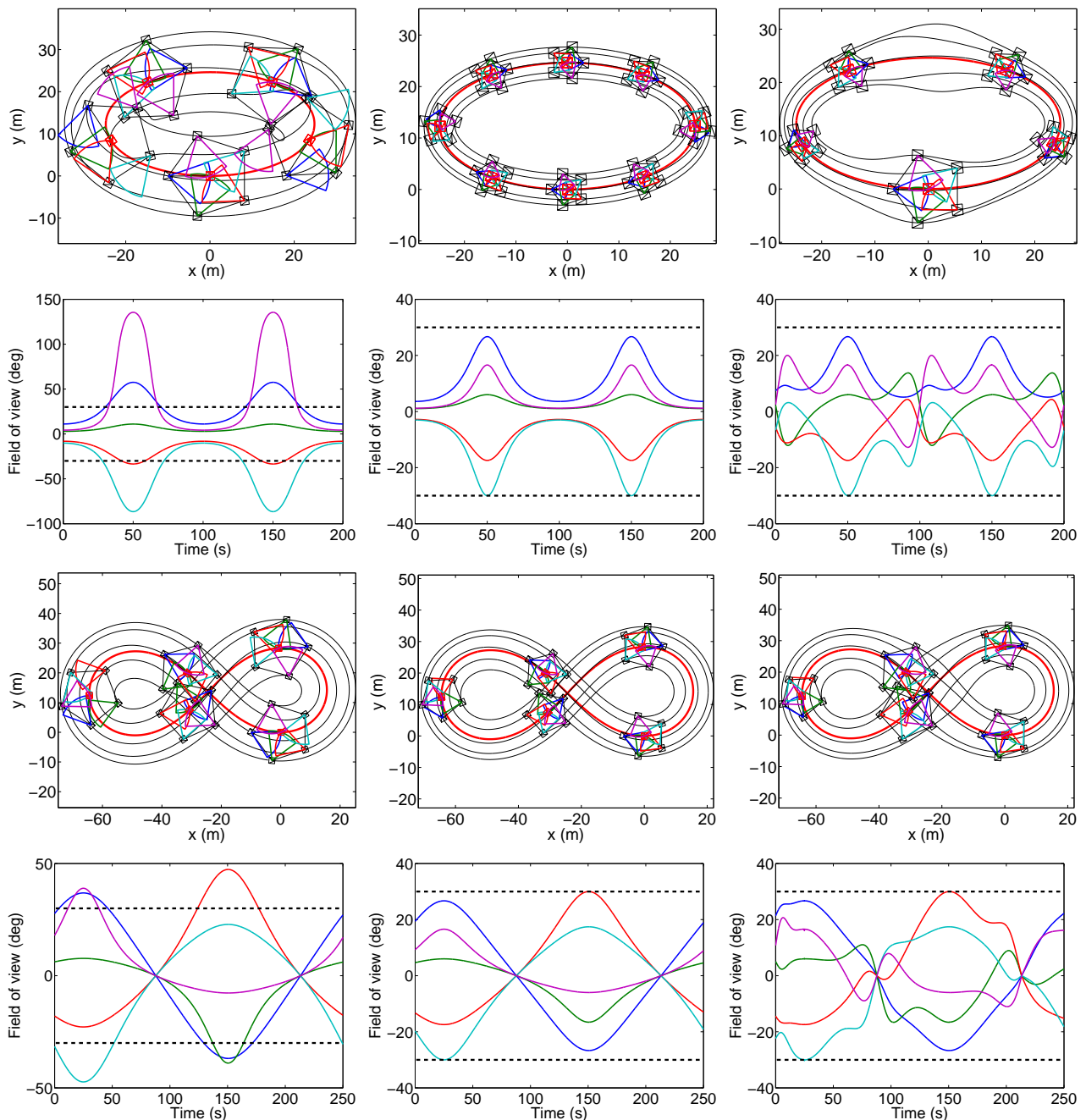


Fig. 2. Simulations enclosing and tracking a target with ellipsoidal motion (first-second row) and 8-shape motion (third-fourth row). Three cases are shown from left to right column: Constant  $d$  not satisfying FOV constraint; constant  $d$  guaranteeing FOV; and maximizing  $d$ . First and third rows: Motion of the target and the enclosing robots. The polygon of the formation and the wedges representing their FOV are shown for some instants of time. Second and fourth rows: target projection angle on each camera along the time. The FOV limits ( $\pm\beta$ ) are depicted as dashed horizontal lines.

FOV constraints (i.e.  $\kappa$  is smaller than the minimum that guarantees FOV constraints). As a result, it can be seen that, although the formation is maintained, the target leaves the FOV of some robots during the tracking. The second case considers constant  $d$  (with  $d = 1/0.31$  for the first example and  $d = 1/0.15$  for the second example) to be the maximum constant value that guarantees FOV constraints (section IV-A). In this case the evolution of the target projection is within the FOV of all the cameras. The third case uses the reference trajectories as defined in section IV-B. The robot velocities of

the first example are also shown in Fig. 3. The evolution of the formation scale for the two strategies presented is shown in Fig. 4. These previous examples are provided in the **video attachment** to better illustrate our proposal.

## VI. CONCLUSIONS

This paper presents the procedure to define appropriate trajectories to enclose and track a moving target with a multi-robot system while obeying motion and FOV constraints. The presented method relies on a formation control formulation

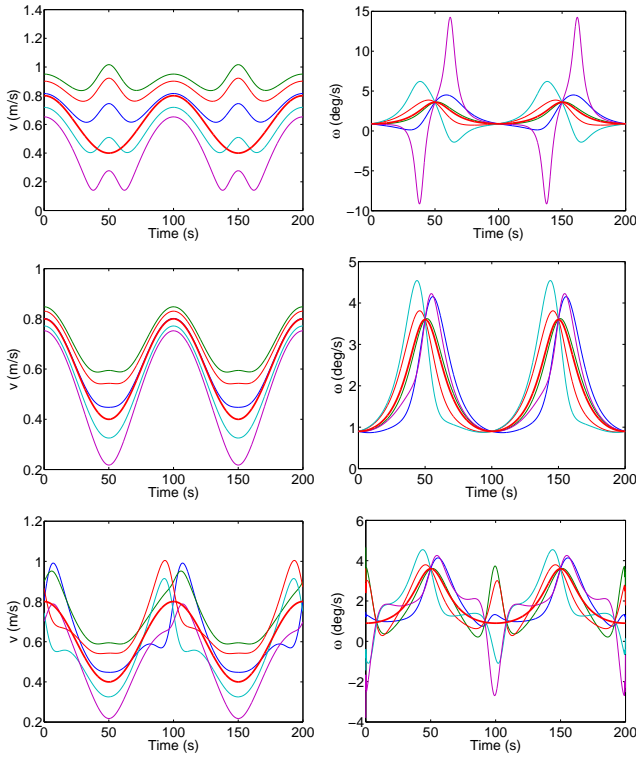


Fig. 3. Robot velocities of the first simulation in Fig. 2 enclosing and tracking a target with ellipsoidal motion. Three cases are shown from first to third row: Constant  $d$  not satisfying FOV constraint; constant  $d$  guaranteeing FOV; and maximizing  $d$ . Left column: Linear velocities  $v_{r_i}$  and  $v_t$  (thicker). Right column: angular velocities  $\omega_{r_i}$  and  $\omega_t$  (thicker) of all the robots.

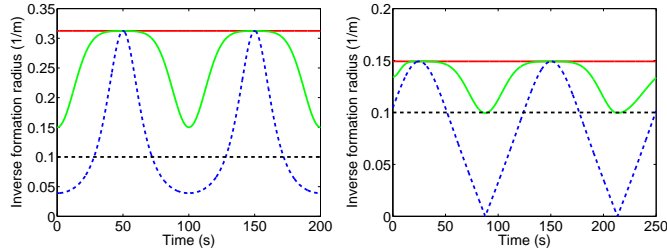


Fig. 4. Evolution of the inverse radius  $\kappa = 1/d$  for first (left) and second (right) example in Fig. 2. Strategy of constant  $d = 10$  m ( $\kappa = 0.1$ ) not satisfying FOV constraint corresponds with the horizontal dashed line. Strategy of constant  $d$  guaranteeing FOV corresponds with the horizontal solid line. Strategy maximizing  $d$  corresponds with the Gaussian-like solid line. The curve in dashed line corresponds to constraint (14).

based on relative position measurements. Then, we assume that each robot is able to compute its relative position with respect to the target from the visual information. It is clear that the robots can implement the strategy we propose using the measurements expressed in their own independent local coordinate frames, without requiring any common reference.

Therefore, our approach does not need global positioning sensors on board the robots, or an external localization system. Moreover, there is no need of communications between the robots and the system is coordinated through the perception of the target, unaware of this. In this paper, we choose circular formations for enclosing the target. Simplicity and lack of occlusions are two of the advantages of this choice.

Notice however that our approach is not restricted to circular formations and can be trivially extended to any kind of formation shape.

## REFERENCES

- [1] G. Antonelli, F. Arrichiello, and S. Chiaverini, "The entrapment/escorting mission," *IEEE Robotics & Automation Magazine*, vol. 15, no. 1, pp. 22–29, 2008.
- [2] R. Sepulchre, D. Paley, and N. Leonard, "Stabilization of planar collective motion: All-to-all communication," *IEEE Transactions on Automatic Control*, vol. 52, no. 5, pp. 811–824, May 2007.
- [3] N. Moshagh, N. Michael, A. Jadbabaie, and K. Daniilidis, "Vision-based, distributed control laws for motion coordination of nonholonomic robots," *IEEE Transactions on Robotics*, vol. 25, no. 4, pp. 851–860, 2009.
- [4] A. Marasco, S. Givigi, and C.-A. Rabbath, "Model predictive control for the dynamic encirclement of a target," in *American Control Conference*, 2012, pp. 2004–2009.
- [5] M. Aranda, G. López-Nicolás, C. Sagüés, and M. M. Zavlanos, "Three-dimensional multirobot formation control for target enclosing," in *2014 IEEE/RSJ International Conference on Intelligent Robots and Systems*, Sept 2014, pp. 357–362.
- [6] Y. Lan, Z. Lin, M. Cao, and G. Yan, "A distributed reconfigurable control law for escorting and patrolling missions using teams of unicycles," in *IEEE Conf. on Decis. and Cont.*, 2010, pp. 5456–5461.
- [7] A. Franchi, P. Stegagno, M. D. Rocco, and G. Oriolo, "Distributed target localization and encirclement with a multi-robot system," in *7th IFAC Symposium on Intelligent Autonomous Vehicles*, 2010.
- [8] K. Zhou and S. I. Roumeliotis, "Multirobot active target tracking with combinations of relative observations," *IEEE Transactions on Robotics*, vol. 27, no. 4, pp. 678–695, Aug 2011.
- [9] P. Tokekar, V. Isler, and A. Franchi, "Multi-target visual tracking with aerial robots," in *2014 IEEE/RSJ International Conference on Intelligent Robots and Systems*, Sept 2014, pp. 3067–3072.
- [10] Z. Wang and D. Gu, "Cooperative target tracking control of multiple robots," *IEEE Transactions on Industrial Electronics*, vol. 59, no. 8, pp. 3232–3240, Aug 2012.
- [11] F. Poiesi and A. Cavallaro, "Distributed vision-based flying cameras to film a moving target," in *2015 IEEE/RSJ International Conference on Intelligent Robots and Systems*, Sept 2015, pp. 2453–2459.
- [12] G. Kantor and A. Rizzi, "Feedback control of underactuated systems via sequential composition: Visually guided control of a unicycle," in *Proc. of 11th Int. Symposium of Robotics Research*, 2003.
- [13] P. Murrieri, D. Fontanelli, and A. Bicchi, "A hybrid-control approach to the parking problem of a wheeled vehicle using limited view-angle visual feedback," *International Journal of Robotics Research*, vol. 23, no. 4-5, pp. 437–448, April-May 2004.
- [14] S. Bhattacharya, R. Murrieta-Cid, and S. Hutchinson, "Optimal paths for landmark-based navigation by differential-drive vehicles with field-of-view constraints," *IEEE Transactions on Robotics*, vol. 23, no. 1, pp. 47–59, 2007.
- [15] P. Salaris, D. Fontanelli, L. Pallottino, and A. Bicchi, "Shortest paths for a robot with nonholonomic and field-of-view constraints," *IEEE Transactions on Robotics*, vol. 26, no. 2, pp. 269–281, April 2010.
- [16] G. Lopez-Nicolas, N. R. Gans, S. Bhattacharya, C. Sagues, J. J. Guerrero, and S. Hutchinson, "Homography-based control scheme for mobile robots with nonholonomic and field-of-view constraints," *IEEE Transactions on Systems, Man, and Cybernetics, Part B (Cybernetics)*, vol. 40, no. 4, pp. 1115–1127, Aug 2010.
- [17] P. Salaris, L. Pallottino, and A. Bicchi, "Shortest paths for finned, winged, legged, and wheeled vehicles with side-looking sensors," *Int. Journal of Robotics Research*, vol. 31, no. 8, pp. 997–1017, 2012.
- [18] J.-B. Hayet, H. Carlos, C. Esteves, and R. Murrieta-Cid, "Motion planning for maintaining landmarks visibility with a differential drive robot," *Robotics and Autonomous Systems*, vol. 62, no. 4, pp. 456–473, 2014.
- [19] M. M. Asadi, A. Ajorlou, and A. G. Aghdam, "Cooperative control of multi-agent systems with limited angular field of view," in *2012 American Control Conference (ACC)*, June 2012, pp. 2388–2393.
- [20] D. Panagou and V. Kumar, "Cooperative visibility maintenance for leader-follower formations in obstacle environments," *IEEE Transactions on Robotics*, vol. 30, no. 4, pp. 831–844, Aug 2014.